

## Band-edge transitions in hexagonal boron nitride epilayers

S. Majety, X. K. Cao, J. Li, R. Dahal, J. Y. Lin et al.

Citation: *Appl. Phys. Lett.* **101**, 051110 (2012); doi: 10.1063/1.4742194

View online: <http://dx.doi.org/10.1063/1.4742194>

View Table of Contents: <http://apl.aip.org/resource/1/APPLAB/v101/i5>

Published by the [American Institute of Physics](#).

---

### Related Articles

Effects of scattering on two-dimensional electron gases in InGaAs/InAlAs quantum wells

*J. Appl. Phys.* **112**, 023713 (2012)

High efficiency ultraviolet emission from Al<sub>x</sub>Ga<sub>1-x</sub>N core-shell nanowire heterostructures grown on Si (111) by molecular beam epitaxy

*Appl. Phys. Lett.* **101**, 043115 (2012)

Current transport in nonpolar a-plane InN/GaN heterostructures Schottky junction

*J. Appl. Phys.* **112**, 023706 (2012)

Superlinear electroluminescence due to impact ionization in GaSb-based heterostructures with deep Al(As)Sb/InAsSb/Al(As)Sb quantum wells

*J. Appl. Phys.* **112**, 023108 (2012)

Analysis of AlN/AlGaN/GaN metal-insulator-semiconductor structure by using capacitance-frequency-temperature mapping

*Appl. Phys. Lett.* **101**, 043501 (2012)

---

### Additional information on *Appl. Phys. Lett.*

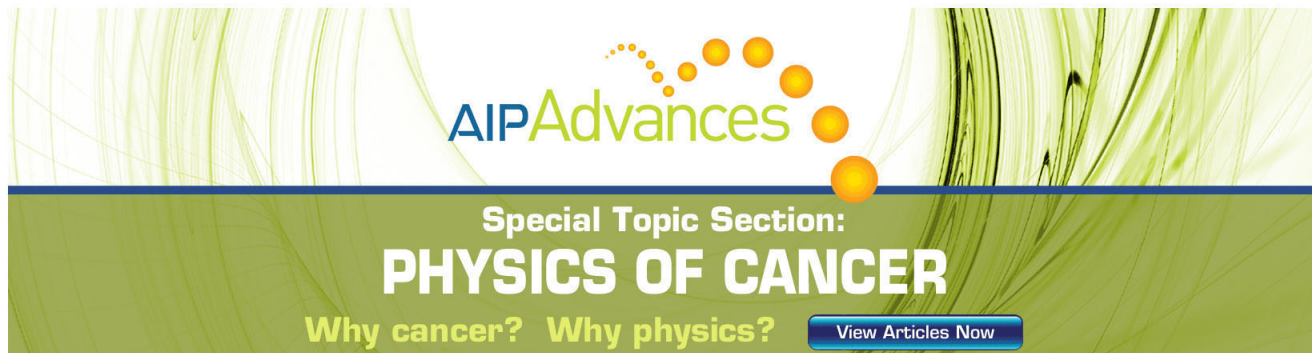
Journal Homepage: <http://apl.aip.org/>

Journal Information: [http://apl.aip.org/about/about\\_the\\_journal](http://apl.aip.org/about/about_the_journal)

Top downloads: [http://apl.aip.org/features/most\\_downloaded](http://apl.aip.org/features/most_downloaded)

Information for Authors: <http://apl.aip.org/authors>

## ADVERTISEMENT

The advertisement features a green and white background with abstract, flowing lines. At the top, the 'AIP Advances' logo is displayed in green and yellow. Below it, the text 'Special Topic Section: PHYSICS OF CANCER' is written in white on a dark green background. At the bottom, the phrase 'Why cancer? Why physics?' is written in yellow, and a blue button with the text 'View Articles Now' is positioned on the right.

AIP Advances

Special Topic Section:  
**PHYSICS OF CANCER**

Why cancer? Why physics? [View Articles Now](#)

## Band-edge transitions in hexagonal boron nitride epilayers

S. Majety, X. K. Cao, J. Li, R. Dahal, J. Y. Lin, and H. X. Jiang<sup>a)</sup>

Department of Electrical and Computer Engineering, Texas Tech University, Lubbock, Texas 79409, USA

(Received 8 May 2012; accepted 19 July 2012; published online 1 August 2012)

Hexagonal boron nitride (hBN) epilayers have been synthesized on sapphire substrates by metal-organic chemical vapor deposition (MOCVD). These MOCVD grown epilayers exhibit highly efficient band-edge photoluminescence (PL) emission lines centered at around 5.5 eV. The results represent a remarkable improvement over the optical qualities of hBN films synthesized by different methods in the past. It was observed that the emission of hBN at 10 K is about 500 times stronger than that of high quality AlN epilayers. Polarization-resolved PL spectroscopy revealed that hBN epilayers are predominantly a surface emission material, in which the band-edge emission with electric field perpendicular to the c-axis ( $\vec{E}_{emi} \perp \vec{c}$ ) is about 1.7 times stronger than the component along the c-axis ( $\vec{E}_{emi} \parallel \vec{c}$ ). This is in contrast to AlN, in which the band-edge emission is known to be polarized along the c-axis, ( $\vec{E}_{emi} \parallel \vec{c}$ ). Time-resolved PL measurements revealed a decay lifetime of around 4.3 ns at 10 K for the dominant band-edge transition line. The present result together with the ability of p-type doping of hBN represents a major step towards the realization of hBN based practical devices. © 2012 American Institute of Physics. [<http://dx.doi.org/10.1063/1.4742194>]

Hexagonal boron nitride (hBN) has attracted much interest, largely because of its potential as a deep-ultraviolet (DUV) photonic material<sup>1–5</sup> and as a substrate and dielectric layer for graphene electronics/optoelectronics.<sup>6–10</sup> Band-edge photoluminescence (PL) properties have been investigated and reported in bulk hBN crystals<sup>1–5</sup> and powders.<sup>11</sup> So far, hBN bulk crystals with size up to millimeters can be grown.<sup>1–5</sup> Other than small size, bulk crystal growth has disadvantages of difficulty to control the growth conditions such as intentional doping and formation of device structures and is most suitable for producing substrates if crystal size can be increased. The synthesis of wafer-scale semiconducting hBN epitaxial layers with high crystalline and optical qualities and electrical conductivity control is highly desirable for the fundamental understanding and the exploration of emerging applications of this interesting material. However, no band-edge photoluminescence emissions have been observed in hBN thin films synthesized previously by various methods.<sup>6,12–15</sup> As with other semiconductor materials in their development stages, realizing the band-edge photoluminescence emission at room temperature is a *prerequisite* in research and *development* towards practical applications of hBN. Metal organic chemical vapor deposition (MOCVD) is a proven technique with the ability to precisely and reproducibly deposit very thin layers (single atomic layers) to thick epilayers (tens of  $\mu\text{m}$  in thickness). Most recently, we have demonstrated the synthesis of wafer-scale semiconducting hBN epitaxial layers with high crystalline quality and p-type conductivity control by *in situ* Mg doping,<sup>16,17</sup> thereby providing an exceptional opportunity to overcome the intrinsic problem of p-type doping in Al-rich AlGaN alloys and enhance to the quantum efficiency of DUV devices. We present here the results of detailed studies of the band-edge transitions in hBN epilayers probed by polarization- and time-resolved PL emission spectroscopy.

Epitaxial layers of hBN employed in this study were produced by MOCVD growth method using triethylboron (TEB) and ammonia ( $\text{NH}_3$ ) as B and N source, respectively. Samples were grown at 1300 °C using hydrogen as a carrier gas with a growth rate of 0.5  $\mu\text{m}/\text{h}$ . The growth rate was observed to be proportional to TEB flow rate. X-ray diffraction (XRD) measurements revealed that the sample employed in this work (1  $\mu\text{m}$  thick hBN on c-plane sapphire) has a full width at half maximum (FWHM) of  $\sim 400$  arcsec for the hBN (0002) rocking curve,<sup>16</sup> which is a dramatic improvement over previously reported values for hBN films (1.5°–0.7°),<sup>14</sup> but is comparable to those of GaN epilayers with a comparable thickness.<sup>18</sup> The PL spectroscopy system consists of a frequency quadrupled 100 fs Ti: sapphire laser with excitation photon energy set around 6.28 eV and a monochromator (1.3 m). A single photon counting detection system together with a micro-channel-plate photo-multiplier tube (with 20 ps time resolution) or a streak camera (2 ps time resolution) was used to record time-resolved PL spectra.<sup>19–21</sup> A high quality and well characterized AlN epilayer (1  $\mu\text{m}$  thick) grown on c-plane sapphire by MOCVD (Refs. 19–21) was used as a reference for comparison PL studies since *wurtzite* AlN has a similar band gap as hBN.

Figure 1 shows the comparison of PL spectra of our hBN and AlN epilayers measured side-by-side at (a) 10 K and (b) 300 (K). A strong band-edge PL emission centered at about 5.48 eV at 10 K was observed in hBN. We notice that the spectral peak position of the free exciton emission line in AlN exhibits a red-shift with increasing temperature, following the bandgap variation with temperature of AlN.<sup>19</sup> For hBN, we are unable to detect the variation of the spectral peak position with temperature. Furthermore, the band-edge PL emission from hBN is more than two orders of magnitude higher than that of AlN, which is considered to be a highly efficient emission material and is the current default choice for DUV device implementation. Several factors may account for this extraordinarily efficient band-edge emission

<sup>a)</sup>Email: hx.jiang@ttu.edu.

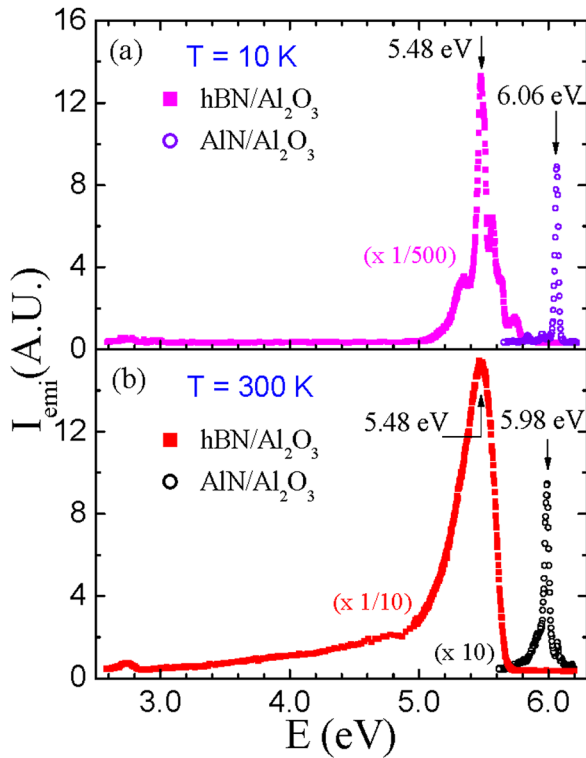


FIG. 1. (a) Low temperature (10 K) and (b) room temperature (300 K) PL spectra of hBN and AlN epilayers grown on sapphire substrate by MOCVD.

in hBN: (1) the high optical absorption coefficient,<sup>22</sup> (2) dominant surface emission of hBN in contrast to dominant edge emission of AlN,<sup>20,21</sup> and (3) layered structure of hBN. Recent theoretical studies have suggested that an efficient band-edge emission is expected from hBN due to its graphite like layered structure and small lattice constant in the c-plane.<sup>23,24</sup> The layer structured hBN provides a natural 2D system, which can result in an increase in the exciton binding energy and oscillator strength over the 3D systems such as AlN.<sup>25</sup>

Figure 2 shows the polarization dependent band-edge PL emission of an hBN epilayer measured at 10 K. The PL emission spectrum line shape for the configuration with emission polarization along the crystal c-axis ( $\vec{E}_{emi} \parallel \vec{c}$ ) is observed to be very similar to that in the  $\vec{E}_{emi} \perp \vec{c}$  configuration. However, we have noticed that the emission intensity is about 1.7 times stronger in  $\vec{E}_{emi} \perp \vec{c}$  configuration, which is similar to some of the well understood semiconductor materials including GaN, however, is in sharp contrast to AlN. It is now a well established fact that the band-edge emission in AlN is polarized along the c-axis, ( $\vec{E}_{emi} \parallel \vec{c}$ ), due to the nature of its band structure (the negative crystal-field splitting in AlN).<sup>20,21</sup> This polarization property of AlN has a profound impact on the device applications. For instance, for UV light emitting diodes (LEDs) using c-plane Al-rich  $Al_xGa_{1-x}N$  as active layers, the most dominant emission will be polarized along the c-axis ( $\vec{E}_{emi} \parallel \vec{c}$ ), which implies that UV photons can no longer be extracted easily from the surface.<sup>21</sup> Thus, incorporating methods for enhancing the light extraction is critical in AlGaN UV LEDs.<sup>26</sup> Furthermore, in contrast to all conventional semiconductor laser diodes with lasing output polarized in the transverse-electric field (TE) mode, it was predicted<sup>21</sup> and experimentally verified<sup>27</sup> that

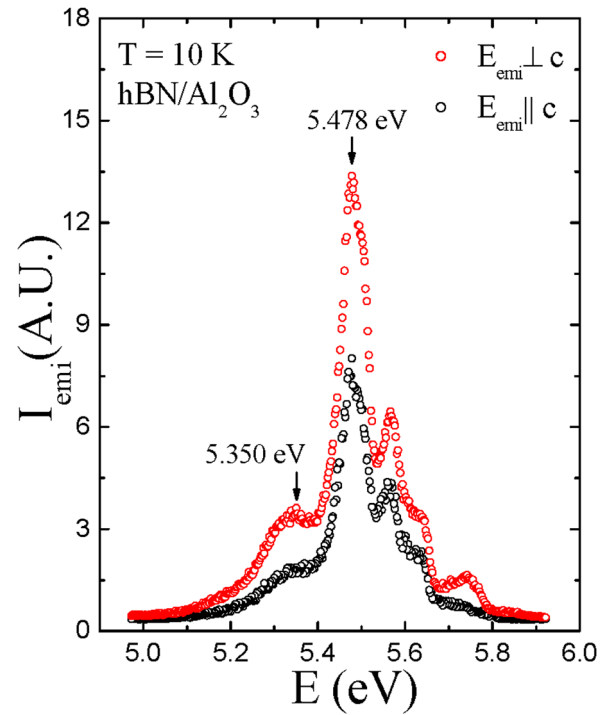


FIG. 2. Low temperature (10 K) band-edge PL spectra of an hBN epilayer with emission polarization parallel ( $\vec{E}_{emi} \parallel \vec{c}$ ) and perpendicular ( $\vec{E}_{emi} \perp \vec{c}$ ) to the c-axis. Excitation laser line is polarized in the direction perpendicular to the c-axis ( $\vec{E}_{exc} \perp \vec{c}$ ).

lasing radiation from c-plane Al-rich  $Al_xGa_{1-x}N$  based laser diodes is strongly polarized in the transverse-magnetic-field (TM) mode. These are currently critical issues facing the development of deep UV light emitting devices based on AlGaIn. Thus, the observed predominant  $\vec{E}_{emi} \perp \vec{c}$  polarization of the band-edge emission in hBN is an advantageous feature over AlN for UV light emitting device applications. In addition, our recent report on the ability of p-type doping of hBN has indicated that a much lower room temperature p-type resistivity (12  $\Omega$ -cm) can be achieved in Mg doped hBN compared to that in Mg doped AlN (>10<sup>7</sup>  $\Omega$ -cm).<sup>16,17</sup> These results together clearly demonstrate that hBN can be a preferred choice as the next generation deep UV photonic material.

In Fig. 3, we fitted the observed low temperature (10 K) PL spectrum with multiple peaks using the Gaussian functions. Six peak fitting reveals the experimentally observed spectrum with the strongest intensity at 5.478 eV and the highest emission spectral peak position at 5.741 eV. These emission lines have been reported previously in bulk and powder hBN and were believed to be due to the recombination of self-trapped excitons.<sup>1-5,11,23</sup> We also observed a peak at 5.350 eV, which was previously assigned to a quasi-donor-acceptor-pair (q-DAP) transition and its peak position red (blue) shifted with a decrease (increase) in temperature (excitation laser intensity).<sup>11,23</sup> The PL emission spectral line shape, including the main 5.478 eV band and minor peak features at 5.509, 5.568, and 5.627 eV are very similar to the diffuse (D) exciton bands reported for a bulk hBN crystal “deformed” by pressure applied by fingers, which possibly induces the BN sp<sup>2</sup> layers gliding.<sup>2-5</sup> The sharp (S) exciton bands<sup>2-5</sup> centered around 5.8 eV emitted from a more perfect hBN crystalline structure are absent. Based on this, we can speculate that the structure of layer stacking of

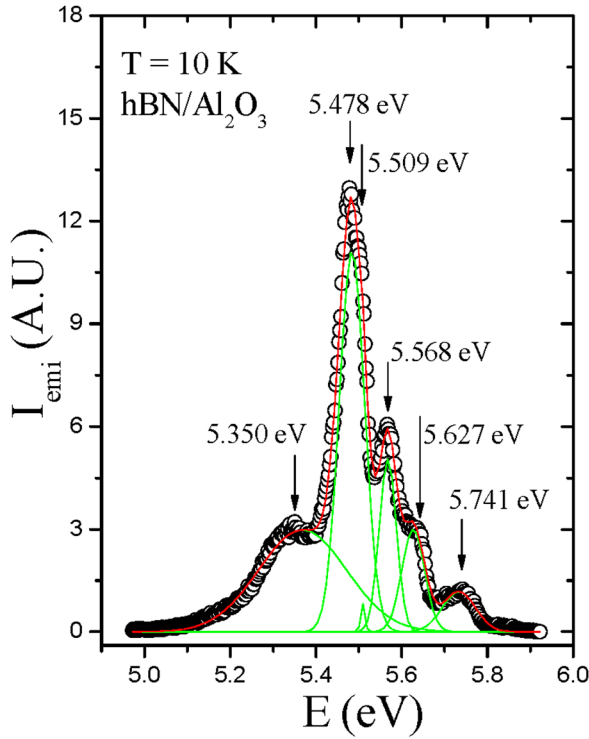


FIG. 3. Low temperature (10 K) band-edge PL spectrum of an hBN epilayer in the energy range of 4.9–6.0 eV. The six fitted Gaussian peaks are plotted in solid lines.

our MOCVD grown hBN epilayers may be similar to that of the deformed bulk hBN crystals. The inherent deformation of hBN epilayers could be due to (1) that the MOCVD growth temperature 1300 °C is still not high enough to allow hBN epilayers to fully crystallize into a more perfect crystalline structure and (2) the presence of strain induced by the heteroepitaxial growth on sapphire substrates.

It was pointed out by a previous calculation that there exists a substable structure of hBN,<sup>28</sup> which corresponds to a glide distance of B-N bond length (1.446 Å) of all B layers of an ABAB... stacking aligning in a direction of in-plane B-N bond, which is a configuration that is quite stable since its total energy is only slightly above the ground state. Most interestingly, though the ground state is indirect, the substable state forms a direct band with an energy gap of about 0.6 eV smaller than that of the ground state (indirect). Although the exact structure of layer stacking of MOCVD grown hBN epilayers is not yet fully understood, the high emission efficiency results shown in Fig. 1 certainly support that hBN epilayers are a direct band gap material.

Figure 4(a) shows the PL decay characteristics of the transition line at 5.478 eV measured at 10 K. The decay kinetics can be approximately described by a single exponential function as illustrated by the solid curve in Fig. 4(a). The measured decay lifetime for the q-DAP transition at 5.35 eV is larger than 20 ns. Long decay time is a characteristic of DAP transition. The decay lifetime ( $\tau$ ) of the 5.478 eV emission line was obtained by fitting data using the following equation:

$$I_{\text{emi}}(t) = A * \exp[-t/\tau], \quad (1)$$

where  $I_{\text{emi}}(t)$  is the emission intensity at decay time  $t$  and  $A$  is the peak intensity at which the decay time is define to be

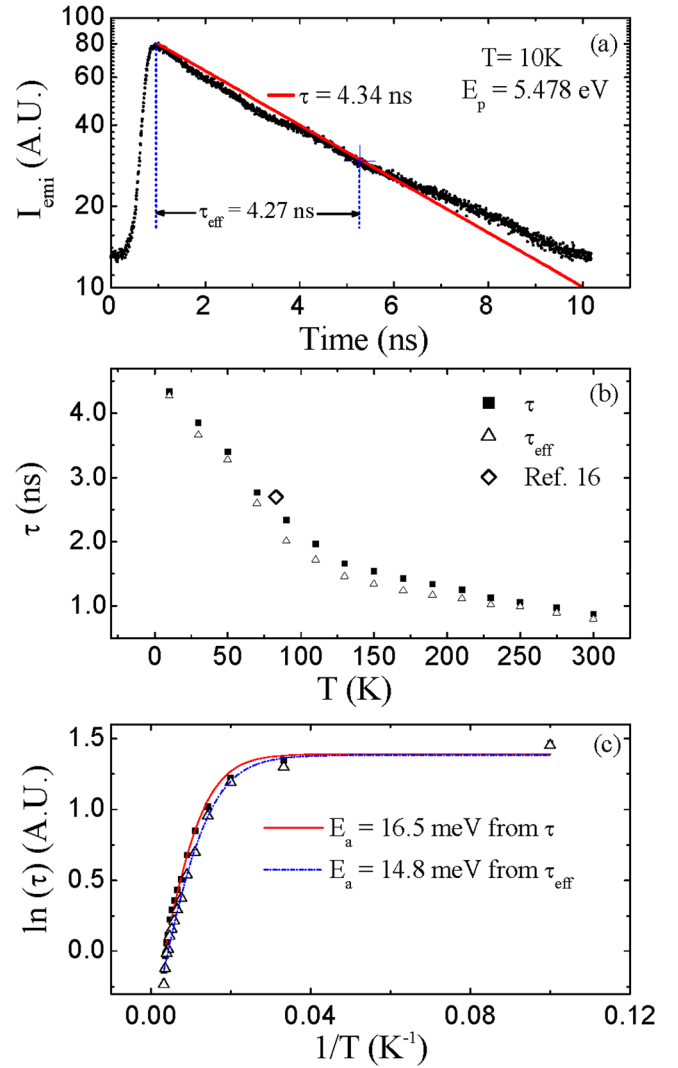


FIG. 4. (a) PL decay characteristics of the 5.478 eV emission line in an hBN epilayer measured at 10 K. (b) Temperature dependent decay lifetime ( $\tau$  and  $\tau_{\text{eff}}$ ) of the 5.478 eV emission line in an hBN epilayer measured from 10 K to 300 K. Open diamond represents a data point measured from bulk hBN (Ref. 2). (c) The Arrhenius plot of the decay lifetime ( $\tau$  and  $\tau_{\text{eff}}$ ) and the data fitted using Eq. (2). The fitted values of activation energy ( $E_a$ ) from  $\tau$  and  $\tau_{\text{eff}}$  are also indicated in the figure.

zero, also known as the prefactor. The measured decay lifetime ( $\tau$ ) from the single exponential fit is about  $\sim 4.34$  ns, as depicted in Fig. 4(a). We have also measured the effective decay lifetime ( $\tau_{\text{eff}}$ ), which is the time it takes for  $I_{\text{emi}}$  to decay from  $A$  to  $A/e$ . The value of  $\tau_{\text{eff}}$  appears to be pretty close to the  $\tau$  value obtained from the single exponential fit.

Figure 4(b) presents the temperature dependence of the decay lifetime ( $\tau$  and  $\tau_{\text{eff}}$ ) of the 5.478 eV emission line measured from 10 to 300 K. The peak position of the emission line changes with temperature. We have measured the decay lifetime at the peak positions at different temperatures. Measured  $\tau$  and  $\tau_{\text{eff}}$  are very consistent in the entire temperature range and comparable to the published results on a deformed bulk crystal of hBN, which exhibited a peak emission at roughly the same energy position with a decay lifetime of about 2.9 ns at 83 K.<sup>11,23</sup> The temperature dependence of  $\tau$  can be described by a thermal activation behavior with an activation energy  $E_a$  of  $\sim 15$  meV as illustrated in

Fig. 4(c). The activation energy was calculated using the equation

$$\tau(T) = \frac{\tau_0}{1 + \alpha \exp(-E_a/k_B T)} \quad (2)$$

where  $\tau(T)$  is the decay lifetime at temperature  $T$ ,  $\tau_0$  is the decay lifetime at temperature  $0\text{K}$ ,  $k_B$  is the Boltzmann constant,  $E_a$  is the activation energy, and  $\alpha$  is a constant. We have obtained  $E_a$  using both the  $\tau$  and  $\tau_{\text{eff}}$  values and found that the  $E_a$  values are quite close in both cases ( $\sim 15\text{meV}$ ) as shown in Fig. 4(c). The physical origin of this activation behavior associated with the decay lifetime is not clear at this stage.

In summary, we have synthesized via MOCVD hBN epilayers with high crystalline and optical qualities. A very efficient PL emission band centered at  $5.478\text{eV}$  with an intensity that is more than two orders of magnitude higher than the free exciton emission in AlN epilayers was observed, which represents a significant improvement over the optical qualities of hBN films synthesized by different methods in the past. Polarization-resolved PL results have revealed that hBN is predominantly a surface emission material with light output polarized in the TE mode. Our results indicate that device quality hBN epilayers can be produced by MOCVD technique. The present results together with the ability of p-type doping of hBN represents a major step towards the realization of hBN based practical devices.

The effort on the fundamental optical studies of hBN is supported by DOE (Grant No. FG02-09ER46552) and the effort of MOCVD growth of hBN is supported by DARPA-CMUVT program (Grant No. FA2386-10-1-4165 managed by Dr. John Albrecht). Jiang and Lin are grateful to the AT&T Foundation for the support of Ed Whitacre and Linda Whitacre endowed chairs. The authors would also like to thank Dr. Ashok Sedhain for his help with the PL measurement system.

<sup>1</sup>Y. Kubota, K. Watanabe, O. Tsuda, and T. Taniguchi, *Science* **317**, 932–934 (2007).

<sup>2</sup>K. Watanabe, T. Taniguchi, T. Kuroda, O. Tsuda, and H. Kanda, *Diamond Relat. Mater.* **17**, 830 (2008).

<sup>3</sup>K. Watanabe, T. Taniguchi, and H. Kanda, *Nature Photon.* **3**, 591 (2009).

<sup>4</sup>K. Watanabe and T. Taniguchi, *Phys. Rev. B* **79**, 193104 (2009).

<sup>5</sup>K. Watanabe and T. Taniguchi, *Int. J. Appl. Ceram. Technol.* **8**, 977 (2011).

<sup>6</sup>L. Song, L. Ci, H. Lu, P. B. Sorokin, C. Jin, J. Ni, A. G. Kvashnin, D. G. Kvashnin, J. Lou, B. I. Yakobson, and P. M. Ajayan, *Nano Lett.* **10**, 3209 (2010).

<sup>7</sup>R. V. Gorbachev, I. Riaz, R. R. Nair, R. Jalil, L. Britnell, B. D. Belle, E. W. Hill, K. S. Novoselov, K. Watanabe, T. Taniguchi, A. K. Geim, and P. Blake, *Small* **7**, 465 (2011).

<sup>8</sup>Y. Shi, C. Hamsen, X. Jia, K. K. Kim, A. Reina, M. Hofmann, A. L. Hsu, K. Zhang, H. Li, Z. Juang, M. S. Dresselhaus, L. J. Li, and J. Kong, *Nano Lett.* **10**, 4134 (2010).

<sup>9</sup>N. Alem, R. Erni, C. Kisielowski, M. D. Rossell, W. Gannett, and A. Zettl, *Phys. Rev. B* **80**, 155425 (2009).

<sup>10</sup>C. R. Dean, A. F. Young, I. Meric, C. Lee, L. Wang, S. Sorgenfrei, K. Watanabe, T. Taniguchi, P. Kim, K. L. Shepard, and J. Hone, *Nature Nanotechnol.* **5**, 722 (2010).

<sup>11</sup>L. Musur and A. V. Kanaev, *J. Appl. Phys.* **103**, 103520 (2008).

<sup>12</sup>K. Nose, H. Oba, and T. Yoshida, *Appl. Phys. Lett.* **89**, 112124 (2006).

<sup>13</sup>B. He, W. J. Zhang, Z. Q. Yao, Y. M. Chong, Y. Yang, Q. Ye, X. J. Pan, J. A. Zapien, I. Bello, S. T. Lee, I. Gerhards, H. Zutz, and H. Hofmann, *Appl. Phys. Lett.* **95**, 252106 (2009).

<sup>14</sup>Y. Kobayashi, T. Akasaka, and T. Makimoto, *J. Cryst. Growth* **310**, 5048 (2008).

<sup>15</sup>Y. Kobayashi, C. L. Tsai, and T. Akasaka, *Phys. Status Solidi C* **7**, 1906 (2010).

<sup>16</sup>R. Dahal, J. Li, S. Majety, B. N. Pantha, X. K. Cao, J. Y. Lin, and H. X. Jiang, *Appl. Phys. Lett.* **98**, 211110 (2011).

<sup>17</sup>S. Majety, J. Li, X. K. Cao, R. Dahal, B. N. Pantha, J. Y. Lin, and H. X. Jiang, *Appl. Phys. Lett.* **100**, 061121 (2012).

<sup>18</sup>S. Nakamura, G. Fasol, and S. J. Pearton, *The Blue Laser Diode: The Complete Story* (Springer, New York, 2000).

<sup>19</sup>K. B. Nam, J. Li, M. L. Nakarmi, J. Y. Lin, and H. X. Jiang, *Appl. Phys. Lett.* **82**, 1694 (2003).

<sup>20</sup>J. Li, K. B. Nam, M. L. Nakarmi, J. Y. Lin, H. X. Jiang, P. Carrier, and S.-H. Wei, *Appl. Phys. Lett.* **83**, 5163 (2003).

<sup>21</sup>K. B. Nam, J. Li, M. L. Nakarmi, J. Y. Lin, and H. X. Jiang, *Appl. Phys. Lett.* **84**, 5264 (2004).

<sup>22</sup>A. Zunger, A. Katzir, and A. Halperin, *Phys. Rev. B* **13**, 5560 (1976).

<sup>23</sup>L. Musur, G. Brasse, A. Pierret, S. Maine, B. Attal-Trétout, F. Ducastelle, A. Loiseau, J. Barjon, K. Watanabe, T. Taniguchi, and A. Kanaev, *Phys. Status Solidi RRL* **5**, 214 (2011).

<sup>24</sup>B. Arnaud, S. Lebègue, P. Rabiller, and M. Alouani, *Phys. Rev. Lett.* **96**, 026402 (2006).

<sup>25</sup>P. K. Basu, *Theory of Optical Processes in Semiconductors: Bulk and Microstructures* (Clarendon Press, Oxford 1997).

<sup>26</sup>J. Shakya, K. H. Kim, J. Y. Lin, and H. X. Jiang, *Appl. Phys. Lett.* **85**, 142 (2004).

<sup>27</sup>H. Kawanishi, M. Senuma, and T. Nukui, *Appl. Phys. Lett.* **89**, 041126 (2006).

<sup>28</sup>L. Liu, Y. P. Feng, and Z. X. Shen, *Phys. Rev. B* **68**, 104102 (2003).